

Narrow-Range Optical pH Sensors Based on Luminescent Europium and Terbium Complexes Immobilized in a Sol Gel Glass

Stephanie Blair, Mark P. Lowe, Celine E. Mathieu, David Parker,*
P. Kanthi Senanayake, and Ritu Katakya

Department of Chemistry, University of Durham, South Road, Durham DH1 3LE, U.K.

Received April 6, 2001

The metal-based emission of a series of luminescent europium and terbium complexes incorporating an aromatic chromophore is rendered pH-dependent either through perturbation of the aryl singlet or triplet energy or by modulating the degree of quenching of the lanthanide excited state. Systems exhibiting each of these pathways have been incorporated in thin-film sol gel matrixes and evaluated as pH sensors in static and flow analyses at constant ionic strength. pH-dependent intensity or ratiometric methods, for emission or excitation spectra, have been defined for lanthanide complexes incorporating substituted phenanthridine (pK_a^* from ca. 6.8 to 7.2) or 6-cyanophenanthridine-2-sulfonyl chromophores ($pK_a \sim 7.14$ in human serum solution) (λ_{exc} 365 nm, $\phi_{H_2O} = 7.2\%$).

Introduction

There have been many advances in the last 20 years in the development of optical methods for signaling changes in pH.^{1,2} Such methods require not only an indicator exhibiting pH-dependent variations in absorption or emission but also the definition of a suitable matrix material to allow the effective immobilization of the indicator. While glass, cellulose, polyurethanes, and polyacrylamides have all been examined, there has been considerable recent interest in the use of sol-gel matrixes because of their advantageous mechanical and chemical stability, optical transparency, and ease of formulation.^{3,4} Several reports have defined the application of sol-gel-based sensors for the analysis of metal ions, anions, oxygen, glucose, and pH.^{5–8} The most common method of indicator entrapment involves chemical doping during formation of the sol-gel glass. Although the covalent linkage of the indicator to a silicon precursor inhibits any problems associated with leaching, there are suggestions that this may be compromised by poorer response times and smaller signal changes.⁹

Luminescent indicators examined to date range from fluorescein derivatives^{1,2} to polyaza transition metal complexes.⁹ However, there are no reports of the use of emissive lanthanide complexes in sol-gel matrixes for this purpose, wherein the metal-based emission from a single-component system reports changes in the analyte concentration. The practical advantages of using the narrow line-like emission from a long-lived Eu or Tb excited state are well-known and have been defined in the

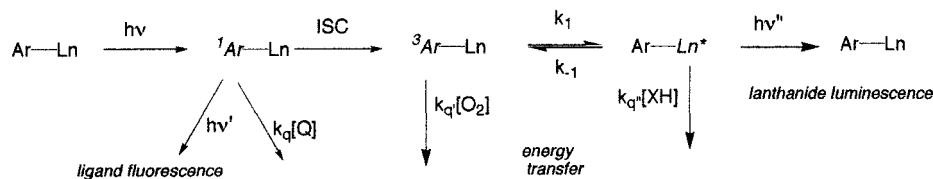
past decade.^{10–12} The generation of a sol-gel thin film requires strongly acidic solvolytic conditions, so that the indicator must be kinetically stable with respect to acid-promoted dissociation. Such stability is a feature of an emerging family of structurally related macrocyclic lanthanide complexes, which possess high chemical stability with respect to decomplexation, may be addressed in the wavelength range 250–390 nm, and exhibit metal-based luminescence which is a defined function of pH, pO_2 , and pX .¹¹ These conjugates, comprising a lanthanide ion strongly bound by a polydentate macrocyclic ligand, incorporate a sensitizing chromophore which serves as an antenna for incident light.

A simple photophysical scheme accounts for their sensitivity to varying concentrations of certain bioactive species^{11,13} (Scheme 1). There are three excited states whose energy or lifetime may be perturbed by varying the concentration of certain ionic or molecular species. Here, it is appropriate to consider only how pH variations lead to modulation of lanthanide luminescence. The energy of the singlet excited state of the integral chromophore may be changed upon protonation of an integral basic site, thereby in principle affecting the sensitivity to competitive quenching (collisional or via photoinduced electron transfer), the rate of intersystem crossing, or the absorption efficiency at a given excitation wavelength. Second, the energy of the intermediate triplet state may be changed by protonation which may modulate the efficiency of intramolecular energy transfer (forward or reverse) to the proximate lanthanide ion. Finally, the excited lanthanide ion itself may be considered: it is subject to competitive vibrational quenching by energy-matched XH oscillators, especially OH and NH groups.^{14,15} If the local coordination environment is rendered pH-dependent in a manner which determines the degree of vibrational quenching, then the lanthanide ion luminescence, in turn, is pH-

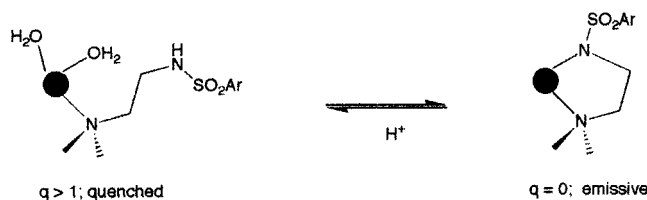
- (1) Wolfbeis, O. S., Ed. *Fibre Optic Chemical Sensors and Biosensors*; CRC Press: Boca Raton, FL, 1991; Vols. 1–2.
- (2) Panova, A. A.; Pantano, P.; Walt, D. R. *Anal. Chem.* **1997**, *69*, 1635.
- (3) Hench, L. L.; West, J. K. *Chem. Rev.* **1990**, *90*, 33.
- (4) Lin, J.; Brown, C. W. *Trends Anal. Chem.* **1997**, *16*, 200.
- (5) Kumov, N. D.; Malhotra, B. D.; Kamalasanan, M. N.; Chandra, S. *Anal. Chem.* **1994**, *66*, 3139.
- (6) McEvoy, A. K.; McDonagh, C.; MacCraith, B. D. *Analyst* **1996**, *121*, 785.
- (7) Wolfbeis, O. S.; Reisfeld, R.; Okhme, I. *Struct. Bonding* **1996**, *85*, 51.
- (8) (a) Malins, C.; Glever, H. G.; Keyes, T. E.; Vos, J. G.; Dressick, W. J.; MacCraith, B. D. *Sens. Actuators* **2000**, *B67*, 89. (b) Lin, J.; Liu, D. *Anal. Chim. Acta* **2000**, *408*, 49.
- (9) Lobnik, A.; Oehme, I.; Murkovic, I.; Wolfbeis, O. S. *Anal. Chim. Acta* **1998**, *367*, 159.

- (10) Mathis, G. *Clin. Chem.* **1995**, *41*, 1391.
- (11) (a) Parker, D. *Coord. Chem. Rev.* **2000**, *205*, 109. (b) Parker, D.; Senanayake, P. K.; Williams, J. A. G. *J. Chem. Soc., Perkin Trans. 2* **1998**, 2129.
- (12) de Silva, A. P.; Fox, D.B.; Huxley, A. J. M.; Moody, T. S. *Coord. Chem. Rev.* **2000**, *205*, 41.
- (13) Clarkson, I. M.; Beeby, A.; Bruce, J. I.; Govenlock, L. J.; Lowe, M. P.; Mathieu, C. E.; Parker, D.; Senanayake, K. *New J. Chem.* **2000**, *24*, 377.

Scheme 1



Scheme 2



sensitive. Such examples have recently been demonstrated,¹⁶ involving a change in hydration state at the Ln ion, as a proximate sulfonamide group reversibly binds in response to pH variation (Scheme 2). We report herein the integration of lanthanide complexes into sol-gel optical sensors exhibiting a pH-dependent emission. Examples operating by each of these pathways are described, and the evaluation of the response characteristics of each sensor in an aqueous flow system is reported.

Lanthanide Complexes: Synthesis and Properties in Homogeneous Solution

The synthesis and characterization of complexes [Ln1] and [Ln2] (Ln = Eu, Tb, Gd) have previously been reported (Chart 1).^{11,13} The introduction of a substituent into the 6-position of the phenanthridine moiety affects the pK_a in a predictable manner, dependent upon the conjugative effect, σ -polarizing influence, or degree of steric congestion imparted. A representative series of 6-substituted phenanthridines was examined with the aim of establishing the protonation constant both in the ground state and in the first excited state (S_1), by observing changes in the absorption and emission spectra as a function of pH (Table 1).¹⁷ Measurements of pK_a were made in a 5:1 mixture of MeOH/H₂O in a fixed salt background (0.1 M NMe₄-ClO₄). Singlet and triplet energies are also collated, determined by examination of absorption spectra at ambient temperature or from phosphorescence spectra in a frozen glass at 77 K. The alkyl substituent enhances the basicity of the nitrogen (compared to phenanthridine itself), and protonation is accompanied by a shift to the red in the absorption maximum of 20 nm and a lowering of the triplet excited state energy by 600 cm⁻¹. A phenyl group at this position is not conjugated significantly with the phenanthridine ring (steric clash with the ring 7-H), and the pK_a was very similar to that of phenanthridine itself. A 6-cyano substituent shifts the absorption maximum to longer wavelength and lowers the triplet energy (λ_{abs} 368 nm), but N-protonation only occurs significantly below pH 2. With this behavior in mind, the lanthanide complexes [Ln.1] and [Ln.2] were considered as suitable for evaluation as "pH indicators"

in a sol-gel matrix. Moreover, the 6-cyanophenanthridine conjugate [Eu.3] was considered as a good choice for assessing the viability of systems operating by on/off sulfonamide ligation (Scheme 2): it absorbs at a relatively long wavelength (up to 390 nm) although the low triplet energy (19600 cm⁻¹) precludes Tb sensitization (⁵D₄ Tb ~ 20400 cm⁻¹; ⁵D₀ Eu ~ 17200 cm⁻¹). For purposes of comparison the analogous arylsulfonamides [Tb.4]⁻ and [Tb.5]⁻ were also evaluated: here the Tb complex is preferred to Eu as higher quantum yields for sensitized Ln emission have been defined.¹³

The synthesis of [Eu.3] required the formation of the *N*-arylsulfonylaziridine, **9**. Chlorination of phenanthridine-6-sulfonic acid, **6**,¹⁸ with POCl₃ afforded the 6-chlorosulfonyl chloride **7** (92%), and subsequent sulfonylation of 2-aminoethanol yielded the sulfonamide **8**, which was transformed into the desired aziridine on treatment with base. Reaction of equimolar quantities of **9** and 1,4,7-tris(*tert*-butoxycarbonylmethyl)-1,4,7,10-tetraazacyclododecane in acetonitrile yielded the *N*-alkylated sulfonamide **10** (69%), and reaction with Ph₃-PNPPh₃CN(PNP⁺CN⁻)¹⁹ in dry MeCN gave the 6-cyano derivative **11** (71%). Deprotection with TFA followed by complexation with EuCl₃ in water allowed the isolation of [Eu.3].

The pH-dependent emission behavior of [Eu.1], [Tb.1], and [Eu.3] was assessed first in aqueous solution. In the case of [Eu.1], the emission profile, following excitation at the isosbestic wavelength 304 nm, mirrored the changes observed by observation of phenanthridine fluorescence and was independent of the degree of sample aeration (λ_{em} 405 nm, $pK_a(S_1) = 5.6 (\pm 0.1)$). As has been discussed in detail elsewhere,¹¹⁻¹³ such behavior reflects the suppression of competitive charge-transfer quenching of the intermediate singlet excited state by the proximate Eu³⁺ ion. The analogous terbium complex, [Tb.1], showed different behavior (Figure 1). In this case, protonation leads to a lowering of the intermediate triplet energy, (Table 1), so that the protonated phenanthridinium triplet is only 600 cm⁻¹ above the Tb ⁵D₄ level and a competitive back-energy transfer process operates (Scheme 1). A detailed analysis of this process has been reported,^{11,13,20} in which the enhancement of the back energy transfer process sets up a photoequilibrium such that the apparent pK_a may reflect the pK_a of the intermediate triplet

(14) Salama, S.; Richardson, F. S. *J. Phys. Chem.* **1980**, *84*, 512. Kropp, J. L.; Windsor, M. W. *J. Chem. Phys.* **1969**, *39*, 2769.

(15) Beeby, A.; Clarkson, I. M.; Dickens, R. S.; Faulkner, S.; Parker, D.; Royle, L.; de Sousa, A. S.; Williams, J. A. G.; Woods, M. *J. Chem. Soc., Perkin Trans. 2* **1999**, 493.

(16) Lowe, M. P.; Parker, D. *Chem. Commun.* **2000**, 707. Lowe, M. P.; Parker, D. *Inorg. Chim. Acta* **2001**, *317*, 163.

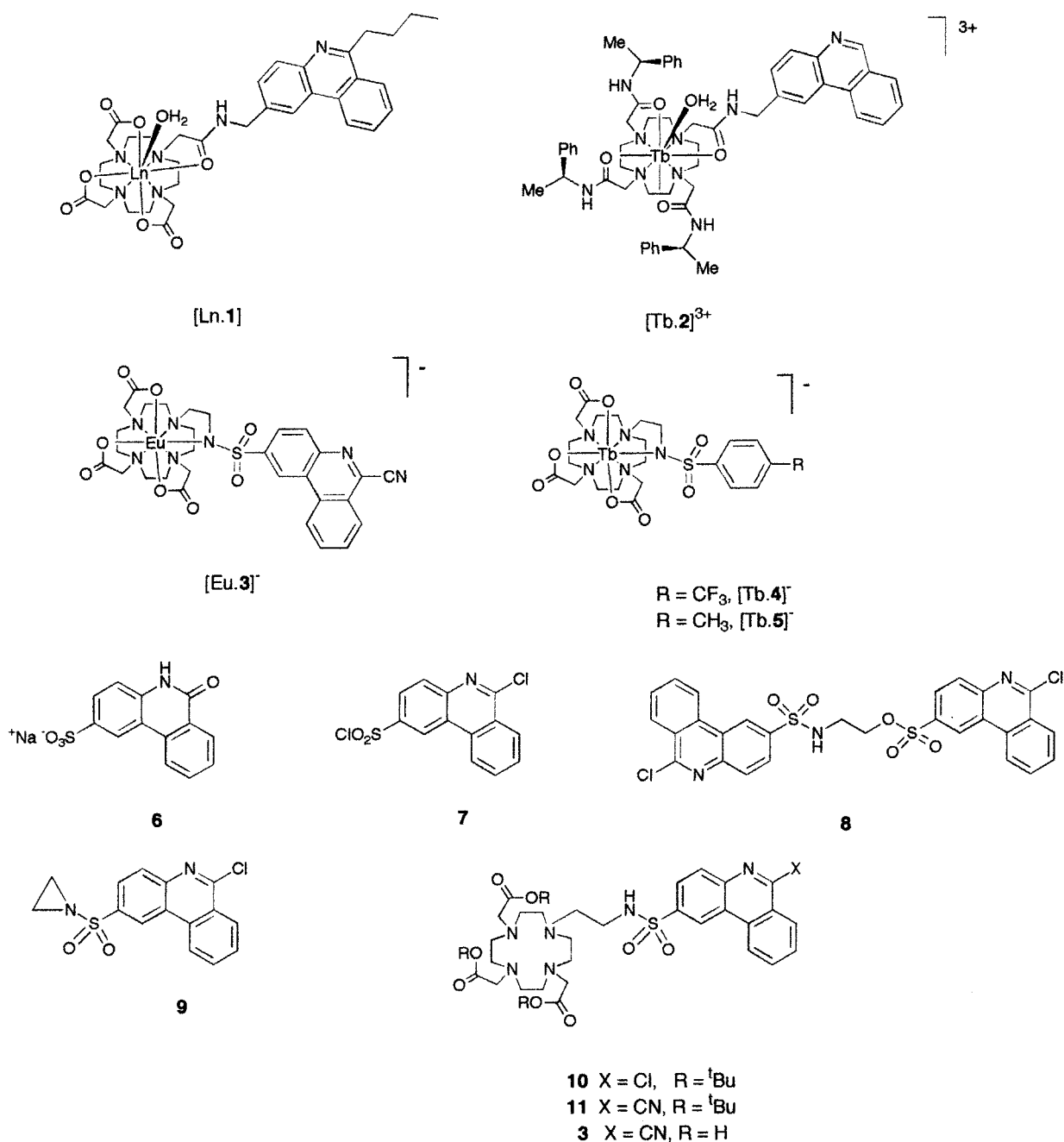
(17) Further examples of 6-substituted phenanthridines are described elsewhere: Mathieu, C. E. Ph.D. Thesis, University of Durham, 2001.

(18) Gilman, H.; Eisch, J. *J. Am. Chem. Soc.* **1957**, *79*, 5479.

(19) Dillon, K. B.; Hodgson, M.; Parker, D. *Synth. Commun.* **1985**, *15*, 849.

(20) Beeby, A.; Faulkner, S.; Parker, D.; Williams, J. A. G. *J. Chem. Soc., Perkin Trans. 2* **2001**, 1268.

Chart 1



state. Accidentally, this may be similar to the singlet pK_a of 5.6 determined from the pH variation of fluorescence (405 nm) for [Tb.1].

With [Eu.3], the absorption spectrum of the 6-CN-phenanthridine chromophore was essentially invariant with pH over the range 10–4. Excitation spectra also were essentially unchanged in form, but reduced dramatically in intensity as the chromophore moved away from the Eu ion following sulfonamide N-protonation.^{†26} Therefore, when exciting [Eu.3] in solution at 385 nm, the observed pH variation (Figure 2) primarily reflects the reduction in the proportion of the more emissive 8-coordinate sulfonamide-bound species, with no change in spectral form. This species possesses no inner-sphere water molecules [$q = 0$; $\varphi_{H_2O} = 7.2\%$ (0.1 M HEPES pH 7.4) (λ_{exc} 385 nm); $\varphi_{D_2O} = 7.9\%$ (pD 7.4)] while the aquated form (>100 times less emissive) is subject to vibrational

quenching by the coordinated OH oscillators.²¹ The measured apparent pK_a of 5.74 (± 0.06) [Figure 2] is directly associated therefore with sulfonamide on/off ligation, i.e., N-protonation. Interestingly, in human serum solution, an apparent pK_a of 7.14 was observed.^{†26} In this case, the complex is likely to bind to the predominant protein serum albumin, with differing affinities for the pendant phenanthridyl moiety (binding more strongly) compared to the more compact sulfonamide-N-bound species, thereby perturbing the observed protonation equilibrium.

Sol-Gel Immobilized Complexes: Sensor Performance

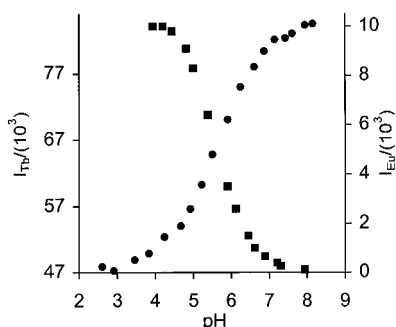
The lanthanide complexes defined above were incorporated into a sol-gel glass matrix and their response characteristics

(21) Infrared analysis of the free ligand and the [Eu.3]⁻ complex (freeze-dried from pH 10) in a KBr matrix revealed no change in the SO₂ vibration at 1325 cm⁻¹, suggesting that no chelation involving the sulfonyl oxygen was occurring.

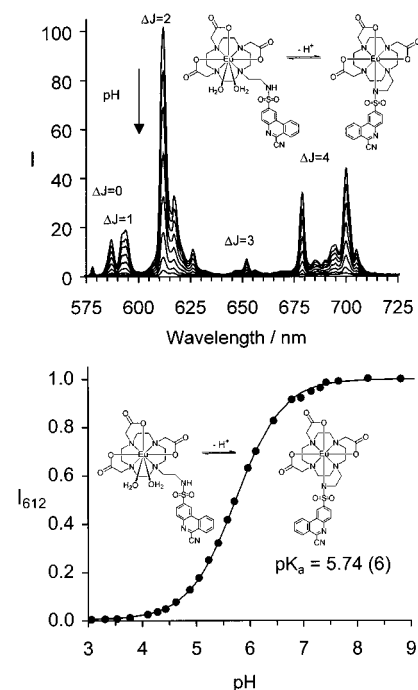
Table 1. Apparent Protonation Constants^a and Singlet and Triplet Excited State Energies^b for a Series of Substituted Phenanthridines and Lanthanide–Phenanthridine Conjugates

compd or complex	E, cm^{-1}		$\text{p}K_{\text{a}} (\pm 0.1)$	
	singlet	triplet	S_0	S_1
6-Bu-phen ^c	28600	21600	4.6	5.0
6-Bu-phenH ⁺	26600	21000		
6-Ph-phen	28200	20700	3.4	3.9
6-Ph-phenH ⁺	26400	20500		
6-CN-phen	27200	21000	<2.5	<2.5
6-CN-phenH ⁺	27200	20400		
[Eu.1]	28800	21700	5.4	5.6
[HEu.1] ³⁺	27300	21100		
[Tb.2] ³⁺	28700	22000	3.3	3.4
[HTb.2] ⁴⁺	27000	21300		
[Eu.3] ^{-d}	26700	19600	<2.5	<2.5

^a Protonation constants for complexes were determined in 0.1 M NMe_4NO_3 (295 K) and for the 6-substituted phenanthridines in 0.1 M NMe_4ClO_4 in 5/1, v/v MeOH/H₂O observing changes in λ_{abs} (365) or λ_{em} (405). ^b Triplet energies were measured at 77 K from phosphorescence spectra in a MeOH/EtOH glass (analogous Gd complexes) or Et₂O/pentane/EtOH glass (aromatics); singlet energies were measured in MeOH/H₂O (5/1) and water for aromatics/complexes, respectively. ^c Under these conditions phenanthridine itself had an apparent $\text{p}K_{\text{a}}$ of 3.4 (S_0) and 3.6 (S_1) and S_1/T_1 energies of 28200, 22000 and 26300, 21300 in its neutral and protonated forms, respectively. ^d Measured in 0.1 M NaCl solution.

**Figure 1.** Comparison of pH–luminescence emission profiles for [Eu.1] (squares) and [Tb.1] (circles) in solution revealing an apparent $\text{p}K_{\text{a}}$ of 5.6 (± 0.1) (295 K, $I = 0.1$ M NMe_4NO_3 , λ_{exc} 308 nm).

studied in both static and flow cells. Details of thin-film fabrication and properties are given in the Experimental Section. Advantage was taken of a modified optical arrangement to enhance sensitivity^{8a,22} (Figure 3). Compared to a simple “face-on” observation set-up, the use of the quartz planar substrate to act as a waveguide coupled to a 90° observation angle led to a 10-fold enhancement of measured signal intensity. Inspection of representative spectra for [Eu.1] immobilized in the silica glass film (Figure 4) revealed the expected pH dependence, with changes in the intensity of emission, but not the form of the emission, occurring. The pH profile for thin films aged for 1, 2, and 3 months revealed relatively little change (Figure 4), with an apparent linear range between pH 8 and 5.5, following excitation at 365 nm. The linear range refers here to the “quasi-linear” region that surrounds the point of inflection. Typical response times (time to attain 95% of the total signal change over the whole range) were of the order of 80–90 s, and baseline drift was not a significant problem (Figure 5). It has been observed previously that the linear range of pH-responsive sol-gel materials is considerably expanded compared to solution, as a result of nonspecific complex/Si–OH interactions.⁸ Moreover, the “apparent” excited state $\text{p}K_{\text{a}}$ of the Eu complex in the

**Figure 2.** Upper: Eu emission spectral response for [Eu.3] as a function of pH in homogeneous solution (295 K, $I = 0.1$ M NaCl, $\lambda_{\text{exc}} = 385$ nm). Lower: Variation of the Eu emission intensity with pH for [Eu.3] in homogeneous solution (0.1 M NaCl, 295 K, $\lambda_{\text{exc}} = 385$ nm), showing the fit (line) to the experimental data with an apparent $\text{p}K_{\text{a}} = 5.74(6)$. In human serum solution, an apparent $\text{p}K_{\text{a}}$ of 7.14(5) was similarly defined (see Supporting Information).

matrix is increased by about 1.5 units compared to solution, consistent with the enhanced polarity of the sol–gel medium. The hypothesis that there exists a matrix of microenvironments for the immobilized Eu complex of differing local acidity and polarity was supported by examination of excitation spectra. Even when the film was exposed to an aqueous solution at pH 9.5, the excitation spectrum revealed a band at 363 nm that was only 25% less intense than when exposed to aqueous solution at pH 4.5, even though the difference in excitation spectral intensity for the corresponding pH values in homogeneous solution was >20:1. Further evidence for the inhomogeneity of complex distribution was provided by examining the characteristics of sensors based on [Tb.1], in sol–gel matrixes where the O/Si ratio was varied from 2 to 4: higher O/Si ratios tend to inhibit indicator leaching,²³ a process which is commonly ascribed to incomplete precursor acid hydrolysis. The sensor prepared with an O/Si ratio of 2 exhibited significantly more baseline drift, and an apparent excited state $\text{p}K_{\text{a}}$ of 8.2 was defined, compared to a $\text{p}K_{\text{a}}$ of 7.2 (Figure 6), for [Tb.1] incorporated in a matrix with a 4/1 O/Si ratio.

The spectral behavior of [Eu.3] when immobilized followed the solution characteristics quite closely: neither the Eu emission lifetime nor the overall spectral form was changed in the N-bound limiting form. An apparent excited state $\text{p}K_{\text{a}}$ of 7.9 (± 0.1) was defined with a 3.5-fold change in intensity at 615 nm (λ_{exc} 330 nm) over the pH range 5–9. Aged samples ($t = 1$ or 3 months) showed no change in the pH profile, and the total emission intensity did not apparently reduce significantly with time, suggesting that leaching or degradation of the complex was not significant.

(22) Gouin, J.-F.; Doyle, A.; MacCraith, B. D. *Electron. Lett.* **1998**, 1685.(23) Butler, T. M.; MacCraith, B. D.; McDonagh, C. J. *Non-Cryst. Solids* **1998**, 224, 249.

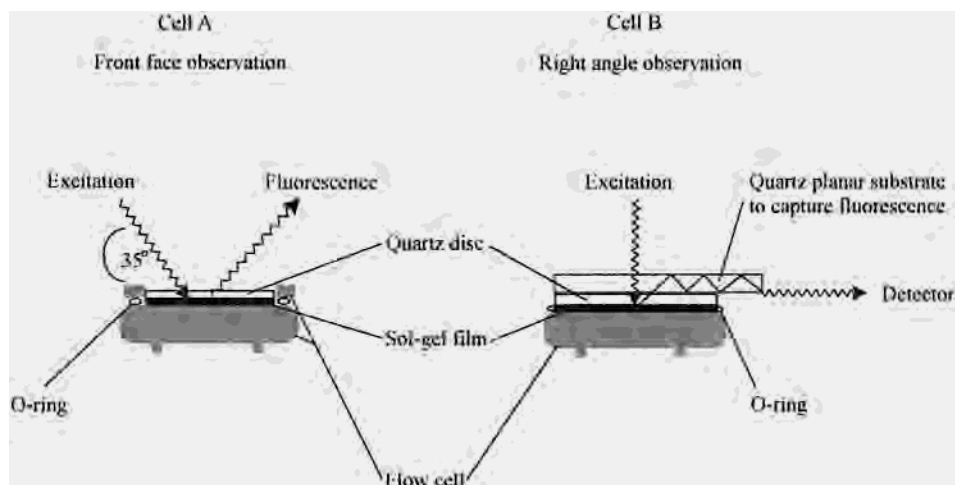


Figure 3. Optical cell arrangements for observation of lanthanide luminescence in a flow-cell. Left: Original design. Right: Modified design with orthogonal observation enhancing sensitivity.

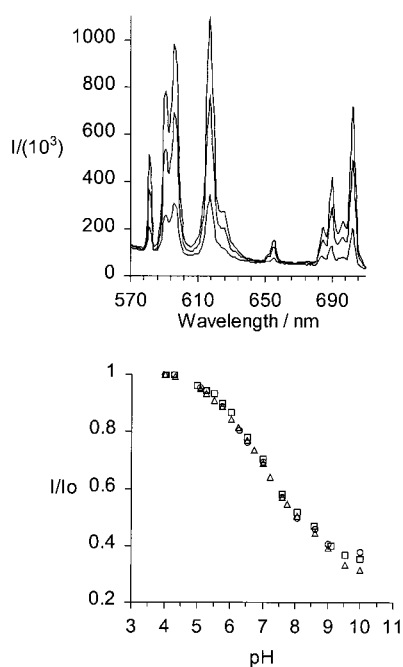


Figure 4. Upper: Variation of europium luminescence intensity for [Eu.1] in a sol-gel membrane at selected pH points (lower pH 4; center pH 7; upper pH 10; $\lambda_{\text{exc}} = 365$ nm, 295 K, $I = 0.1$ M NaCl). Lower: Response of Eu emission intensity ($\lambda_{\text{em}} 616$ nm, $\lambda_{\text{exc}} 365$ nm) as a function of pH for a stabilized sol-gel film containing [Eu.1] (squares) and after aging for a further 1 month (triangles) and 2 months (circles), showing the near linearity of response over the pH range 5.5–8.

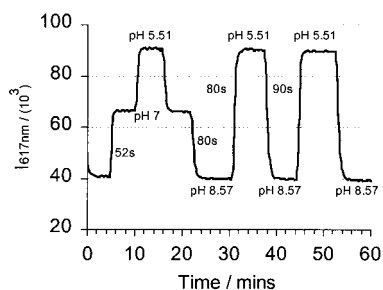


Figure 5. Response time and reversibility behavior for a sol-gel sensor incorporating [Eu.1] in a flow cell, with a stepped pH variation.

Ratiometric Sensors

While sensors operating via variations in emission intensity are very useful, calibration is required prior to usage. If the

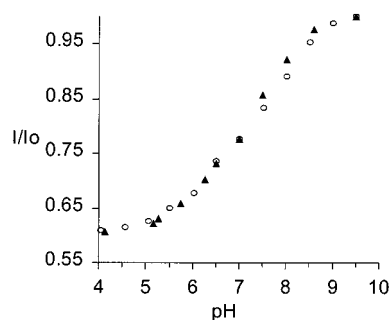


Figure 6. Variation of Tb emission intensity in a stabilized sol-gel (O/Si = 4) containing [Tb.1] ($\lambda_{\text{em}} 544$, $\lambda_{\text{exc}}^{\text{isos}} = 311$ nm) as a function of pH in a flow cell ($I = 0.1$ M NaCl, 295 K), after 1 month (circles) and 2 months (triangles), revealing an apparent $\text{p}K_{\text{a}}$ of 7.2 (± 0.1).

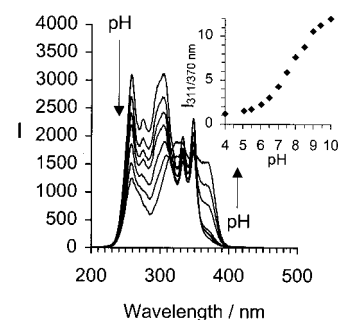


Figure 7. Change in the ratio of excitation bands as a function of pH [$I(\lambda = 311)/I(\lambda = 370)$] for a sol-gel film incorporating [Tb.2]³⁺ ($\text{CF}_3\text{-SO}_3$)₃ ($I = 0.1$ M NaCl; $\lambda_{\text{em}} 548$ nm).

spectral form changes, however, then the ratio of two selected wavelengths may change as a function of pH. Such a variation may be monitored by analyzing either the emission or excitation spectrum. Examples of such behavior have been identified with sensors based on [Tb.2]³⁺ and for [Tb.4] and [Tb.5]. The sol-gel thin film based on the tripositive terbium complex revealed a series of excitation spectra that was much more reminiscent of the corresponding solution spectra. Excitation spectra ($\lambda_{\text{em}} = 548$ nm) at pH 2 and 9 were compared (Figure 7), and although a small long-wavelength tail (>370 nm) is still apparent at pH 9, this is dramatically less pronounced than with the neutral complexes, e.g., [Eu.1], described above. The ratio of the excitation wavelengths at 311 nm (isosbestic wavelength) to 370 nm was therefore plotted as a function of pH and revealed

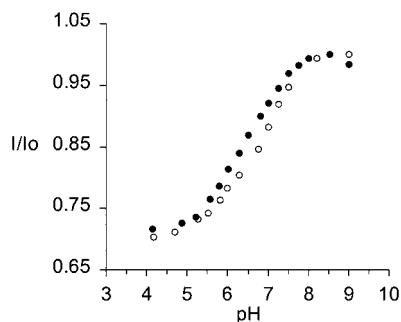


Figure 8. Influence of ionic strength on the apparent protonation constant for [Tb.4] in a sol-gel film (295 K, λ_{em} 544 nm, λ_{exc} = 265 nm), showing apparent pK_a values of 6.8 (I = 20 mM NaCl, filled circles) and 6.4 (I = 100 mM NaCl, open circles).

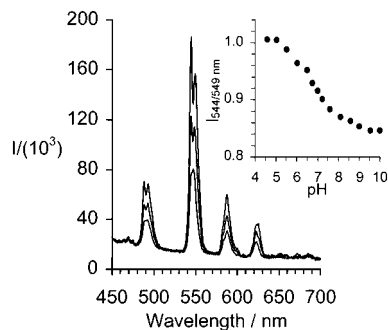


Figure 9. pH dependence of the terbium emission intensity ratio for [Tb.5] in a sol-gel film [λ_{em} = 544)/(λ_{em} = 549 nm); λ_{exc} = 265 nm; 295 K; I = 0.1 M NaCl].

an 8-fold increase over the pH range 4–8 and a 100% increase over the pH range 6.5–7.5 (I = 0.1 M NaCl, 295 K).

A second example of a ratiometric probe was provided by the sol-gel sensors incorporating [Tb.4] and [Tb.5]. These sensors exhibited response times of the order of 100 s, with apparent excited state pK_a values (associated with sulfonamide N-protonation) of 6.3 and 7.2 (295 K, I = 0.1 M NaCl), respectively, compared to values of 5.7 and 6.4 reported in homogeneous solution under identical conditions.¹⁶ The influence of ionic strength on the apparent excited state pK_a was briefly assessed by examining the behavior in 0.1 M NaCl and in a 0.02 M NaCl background. Apparent protonation constants of 6.4 and 6.8 respectively were found (Figure 8), consistent with the enhanced stabilization of the anionic (sulfonamide N-bound) species at the higher ionic strength. Their spectral response was identical both in 0.1 M NaCl (pH 7.4) solution and in a solution containing potential interferent anions (pH 7.4; 30 mM NaHCO_3 , 2.3 mM Na lactate, 0.9 mM NaH_2PO_4 , 0.13 mM Na citrate, 0.1 M NaCl), consistent with the absence of competitive anion binding at the coordinatively “unsaturated” Tb center.²⁴ Terbium emission spectra are inherently complex, as a consequence of the multitude of allowed transitions from the sublevels of the 5D_4 excited state to the 7F_n ground state manifold. However, shift pH-dependent changes were discerned in several bands for [Tb.5] including the $\Delta J = -1$ bands, around 540–550 nm. The variation of the ratio of the emission intensity at 540–550 nm was plotted as a function of pH and showed a modest 20% decrease over the pH range 5–7.5 (Figure 9).

Conclusions

The series of sol-gel thin-film sensors, prepared under acidic hydrolytic conditions incorporating various kinetically stable lanthanide complexes, show well-defined pH-dependent lanthanide emission behavior with response times of about 100 s. The sensors appear to be quite robust with respect to complex leaching and photodegradation. Both intensity-based and ratiometric sensors have been defined with excitation wavelengths in the range 255–385 nm. The enhanced local acidity of the sol-gel medium suggests that systems exhibiting apparent pK_a values in homogeneous solution of around 4.5–6.5 may be particularly appropriate for use in the pH range 6–8.

Experimental Section

Reagents and Solvents. Acetonitrile was dried over calcium hydride before use. Water and H_2O refer to high-purity water with conductivity $\leq 0.04 \mu\text{S cm}^{-1}$, obtained from the PURITE purification system. 1,4,7-Tris(*tert*-butoxycarbonylmethyl)-1,4,7,10-tetraazacyclododecane²⁴ and PNP cyanide¹⁹ were synthesized via published procedures.

Chromatography. Column chromatography was carried out using “gravity” silica (Merck). Cation exchange chromatography was performed using Dowex 50W 50x4-200 strong ion exchange resin, which had been pretreated with 3 M HCl.

Spectroscopy. ^1H NMR spectra were recorded at 299.91 MHz on a Varian Unity-300. ^{13}C NMR were recorded on a Varian Unity-300 at 75.4 MHz. Mass spectra were recorded using a VG Platform II electrospray mass spectrometer with methanol as a carrier solvent. Accurate masses were determined at the EPSRC National MS Service at Swansea; isotope calculations for Eu complexes refer to ^{153}Eu . Luminescence measurements (including quantum yield determinations) for europium complexes were made using an SA Fluorolog 3-11 instrument using DataMax for Windows v2.1. Second-order diffraction effects were obviated by using a 475 nm cutoff filter. Triplet energies were measured at 77 K on a Perkin-Elmer LS 50B equipped with a cryostat. Ultraviolet absorbance spectra were recorded on a Unicam UV2 spectrometer operating with Vision software.

pH measurements were made using a Jenway 3320 pH meter (fitted with a BDH glass + combination electrode-microsample) calibrated with pH 4, 7, and 10 buffer solutions.

pH Titrations. Luminescence pH titrations were carried out in a background of constant ionic strength (I = 0.1 M NaCl, 295 K) or in reconstituted lyophilized human serum on solutions with absorbances of < 0.3 at wavelengths $\geq \lambda_{ex}$ in order to avoid any errors due to the inner filter effect. Solutions were made basic by addition of 1 M NaOH and titrated to acidic pH using small aliquots (typically 0.5 μL) of 1 M or 0.1 M HCl. The luminescence spectra were recorded at each point (30–40 points per titration). Excitation wavelengths of 365 or 385 nm (sensitization via phenanthridinyl chromophore) were used to obtain the luminescence spectra. Excitation and emission slits were 2–5 and 1 nm bandpass, respectively. Points were recorded at 1 nm intervals with a 0.25 s integration time.

Standard least-squares fitting techniques were used to determine protonation constants from the luminescence intensity data.

Quantum Yield Determinations. Measurements were on solutions at pH 7.4 in 0.1 M HEPES buffer and were made relative to two known standards for europium, Rhodamine 101 in ethanol (ϕ = 1) and Cresyl Violet in methanol (ϕ = 0.54). These standards were chosen as they emit in a similar spectral window to europium and possess a similar absorbance to the aromatic antenna at the excitation wavelength in the studied complex. For each of the standards and the unknown, five solutions with absorbances between 0.02 and 0.1 were used. For each of these solutions the absorbance at the excitation wavelength (300 and 370 nm used, both give same values for ϕ) and the total integrated emission intensity were determined.

Sodium 2-Phenanthridinonesulfonate (6). This compound was synthesized using the literature procedure¹⁸

^1H NMR (CD_3OD , 300 MHz, δ): 7.39 (1H, d, 3J = 8.7, H_{10}), 7.69 (1H, t, 3J = 8.1, H_8), 7.92 (2H, t + d, H_9 + H_7), 8.41 (1H, d, 3J = 8.1,

(24) Bruce, J. I.; Dickins, R. S.; Govenlock, L. J.; Gunnlaugsson, T.; Lopinski, S.; Lowe, M. P.; Parker, D.; Peacock, R. D.; Perry, J. J. B.; Aime, S.; Botta, M. *J. Am. Chem. Soc.* **2000**, *122*, 9674.

$^4J = 1.2$, H₃), 8.47 (1H, d, $^3J = 8.1$, H₄), 8.79 (1H, d, $J = 1.2$, H₁). ESMS: m/z 274 (M⁻).

6-Chloro-2-chlorosulfonylphenanthridine (7). The sodium salt **6** was converted to its protonated form by addition of 1 equiv of concentrated hydrochloric acid; the resultant suspension was dried under vacuum. The chlorophenanthridinone sulfonic acid (4.0 g, 14.5 mmol) was treated with phosphorus oxychloride (30 mL), and the suspension was heated at 120 °C for 2 h. Excess phosphorus oxychloride was removed under reduced pressure, and the residue was taken into dichloromethane (50 mL), washed with water (2 × 30 mL), and dried with sodium sulfate. Solvent was removed under reduced pressure to afford a white solid (4.2 g, 92%). Mp: 145–146 °C. Anal. Calcd for C₁₃H₉NO₂SCl₂: C, 50.1; H 2.26, N, 4.48. Found: C, 49.9; H, 2.62; N, 4.76. ESMS+: m/z 313; 335 [M + H]⁺; [M + Na]⁺. ¹H NMR (CDCl₃, 300 MHz, δ): 7.89 (1H, t, $^3J = 7.5$, H₉), 8.01 (1H, t, $^3J = 7.5$, H₈), 8.28 (2H, d + d, H₇ + H₁₀), 8.53 (1H, d, $^3J = 8.1$, H₃), 8.65 (1H, d, $^3J = 8.1$, H₄), 9.17 (1H, s, H₁).

N-(6-Chloro-2-phenanthridinylsulfonyl)aziridine (9). A chilled solution of 2-aminoethanol (0.097 g, 0.0015 mol) in pyridine (1 mL) was added dropwise to a solution of **7** (0.94 g, 0.003 mol), in pyridine (5 mL) at -30 °C. After the addition the temperature was maintained at -10 °C for 1 h. The solution was kept at ~0 °C overnight. The cold solution was poured onto a solution of ice/water to give a yellow precipitate. The solid was filtered and washed with water, dissolved in chloroform, washed with water again (3 × 10 mL), and dried with sodium sulfate, and solvent was removed to give a pale yellow solid. The solid was dissolved in hot chloroform, and ¹H NMR and ESMS analysis revealed the presence of the desired phenanthridinesulfonamide **8**. The product was used without further purification. ESMS+: m/z 614 [M + H]⁺, 636 [M + Na]⁺. ¹H NMR (CDCl₃, 300 MHz) (partial): δ 3.34 (2H, br s, N-CH₂), 4.21 (2H, br s, O-CH₂), 6.32 (1H, br t, NH).

The crude mixture was suspended in toluene (10 mL) and aqueous potassium hydroxide (2 mL, 6 M) and stirred for 3–4 h. The organic layer was separated and dried over potassium carbonate, and solvent was removed to give the desired product as a pale yellow solid (260 mg, 60%). Mp: 134–135 °C. Anal. Calcd for C₁₅H₁₁N₂O₂SCl: C, 56.51; H, 3.48; N, 8.79. Found: C, 56.49; H, 3.49; N, 8.76. ESMS+: m/z 319 [M + H]⁺. ¹H NMR (CDCl₃, 300 MHz, δ): 2.43 (4H, s, CH₂-CH₂), 7.82 (1H, t, $^3J = 9$, ArH), 7.95 (1H, t, $^3J = 9$, ArH), 8.17 (2H, s, ArH), 8.46 (1H, d, $^3J = 9$, ArH), 8.62 (1H, d, $^3J = 9$, ArH), 9.08 (1H, s, ArH). ¹³C NMR (CDCl₃, 300 MHz, δ): 32.50 (CH₂ N), 127.25 (ArCH), 128.11, (ArCH), 128.59 (ArC), 129.9 (ArC), 131.93 (ArCH), 132.71 (ArCH), 134.16 (ArCH), 135.17 (ArCH), 137.38 (ArCH), 138.56 (ArC), 141.02 (ArC), 150.18 (ArC), 159.58 (C-Cl).

1-[2'-(6-Chlorophenanthridinyl-2-sulfonylamino)ethyl]-4,7,10-tris(tert-butoxycarbonylmethyl)-1,4,7,10-tetraazacyclododecane (10). A solution containing 1,4,7-tris(tert-butoxycarbonylmethyl)-1,4,7,10-tetraazacyclododecane (0.092 g, 0.179 mmol), *N*-(6-chlorophenanthridinyl-2-sulfonyl)aziridine **9**, (0.060 g, 0.189 mmol) and Na₂CO₃ (0.019 g, 0.179 mmol) in dry acetonitrile (15 mL) was heated at reflux for 2 days. The reaction mixture was filtered and the solvent removed under reduced pressure. Column chromatography on silica [gradient elution, CH₂Cl₂ to 4% MeOH-CH₂Cl₂, $R_f = 0.27$ (10% MeOH-CH₂-Cl₂)] yielded **10** as a pale yellow oil (0.108 g, 69%). ESMS+: m/z 833 [M + H]⁺. ¹H NMR (300 MHz, CDCl₃, δ): 9.28 (1H, s, ArH), 8.90 (1H, d, ArH), 8.41 (1H, d, ArH), 8.08 (2H, m, ArH), 7.94 (1H, t, ArH), 7.76 (1H, t, ArH), 7.36 (1H, t, NH), 3.60–2.20 (26H, br, CH₂N), 1.39 (27H, s, C(CH₃)₃). ¹³C NMR (75.4 MHz, CDCl₃, δ): 172.9, 172.6 (CO₂), 154.2, 144.8, 137.9, 134.2, 132.8, 129.9, 129.3, 127.6, 126.7, 125.0, 124.3, 123.7, 123.2 (Ar), 82.6, 82.3 (C(CH₃)₃), 56.5, 55.4, 53.2, 50.4 (br), 41.1 (CH₂N), 28.0 (C(CH₃)₃).

1-[2'-(6-Cyanophenanthridinyl-2-sulfonylamino)ethyl]-4,7,10-tris(tert-butoxycarbonylmethyl)-1,4,7,10-tetraazacyclododecane (11). A solution containing **10** (0.040 g, 0.048 mmol) and PNP cyanide (0.034 g, 0.060 mmol) in dry acetonitrile (8 mL) was heated at reflux for 18 h. The solvent was removed under reduced pressure. Column chromatography on silica [gradient elution, CH₂Cl₂ to 5% MeOH-CH₂Cl₂, $R_f = 0.27$ (10% MeOH-CH₂Cl₂)] yielded **11** as a pale yellow oil (0.028 g, 71%). ESMS+: m/z 824 [M + H]⁺. ¹H NMR (300 MHz, CDCl₃, δ): 9.76 (1H, s, ArH), 9.23 (1H, d, ArH), 8.38 (1H, d, ArH), 8.12

(2H, m, ArH), 8.03 (1H, d, ArH), 7.93 (1H, d, ArH), 7.60 (1H, t, NH), 3.60–2.20 (26H, br, CH₂N), 1.40 (27H, s, C(CH₃)₃). ¹³C NMR (75.4 MHz, CDCl₃, δ): 172.6, 172.0 (CO₂), 145.2, 141.8, 138.0, 133.9, 133.6, 133.0, 131.2, 127.8, 126.4, 125.8, 124.9, 124.0 (Ar), 115.8 (CN), 82.5, 82.3 (C(CH₃)₃), 56.6, 55.8, 54.0, 52.2 (br), 41.9 (CH₂N), 28.1, 28.0 (C(CH₃)₃).

1-[2'-(6-Cyanophenanthridinyl-2-sulfonylamino)ethyl]-4,7,10-tris(carboxymethyl)-1,4,7,10-tetraazacyclododecane (3). A solution containing the **11** (0.053 g, 0.064 mmol) in 80% trifluoroacetic acid-CH₂Cl₂ (10 mL) was stirred for 4 h. Solvents were removed under reduced pressure followed by the addition and then evaporation of CH₂-Cl₂ (3 × 10 mL) and finally ether (10 mL). The residue was taken up in H₂O, filtered, and lyophilized to give a pale yellow solid of the tris-trifluoroacetate salt (0.044 g, 77%). Anal. Calcd for C₃₆H₄₀N₇O₁₄F₆S₁: C, 43.3; H, 4.04; N, 9.83. Found: C, 43.1; H, 3.97; N, 9.56. ESMS+: m/z 656 [M + H]⁺. ¹H NMR (300 MHz, D₂O, δ): 8.12 (1H, s, ArH), 7.49 (1H, t, ArH), 7.45 (2H, t, ArH), 7.41 (1H, d, ArH), 7.33 (1H, t, ArH), 7.23 (1H, t, ArH), 3.80–2.90 (26H, br, CH₂N). ¹³C NMR (75.4 MHz, D₂O, δ): 175.8, 175.3 (CO₂), 145.2, 141.5, 136.7, 133.6, 133.5, 133.4, 129.2, 128.5, 125.9, 125.8, 124.6, 121.3 (Ar), 116.7 (CN), 56.6, 55.2, 51.9 (br), 51.8, 40.8 (CH₂N). UV (H₂O) [λ_{\max} nm (ϵ M⁻¹cm⁻¹): 326 (7240), 365 (1820), 385 (1085)].

Europium (III) 1-[2'-(6-Cyanophenanthridinyl-2-sulfonylamino)ethyl]-4,7,10-tris(carboxymethyl)-1,4,7,10-tetraazacyclododecane (Eu.3). An aqueous solution (6 mL) containing **3** (15 mg, 15 μ mol) and EuCl₃·6H₂O (9 mg, 25 μ mol) was adjusted to pH 5.5 using 1 M NaOH and heated at 90 °C for 18 h. On cooling, the pH was raised to 10.0 and the solution filtered through a Celite plug to remove the excess europium as Eu(OH)₃. The pH was then lowered to 5.0 and the solution lyophilized. The compound was extracted from the salt residues with 10% MeOH-CH₂Cl₂ and filtered and the solvent removed under reduced pressure. The residue was taken up in water and lyophilized to give a pale yellow solid (10 mg, 83%). HR ESMS-: m/z [M - H]⁻ calcd for C₃₀H₃₃N₇O₈S₁Eu₁ 804.1324, found 804.1321. ¹H NMR (300 MHz, D₂O, pD = 9, 277 K, δ): partial assignment 33.7 (1H, s, ring CH axial), 27.5 (1H, s, ring CH axial), 25.6 (1H, s, ring CH axial), 17.6 (1H, s, ring CH axial), typical of a monocapped square-antiprismatic geometry about Eu, the remaining resonances span 9.4 to -31.0 ppm. UV (H₂O) [λ_{\max} nm (ϵ M⁻¹ cm⁻¹): 326 (5360), 365 (1500), 385 (680)].

Sol-Gel Film Fabrication. The silicon alkoxide precursor tetramethoxysilane (TMOS) was purchased from Aldrich, and the polished quartz disks (25 mm diameter, 2 mm thickness) were purchased from Multilab, Newcastle-upon-Tyne, U.K. The standard film fabrication process involved mixing TMOS with methanol and acidified water (using HCl as catalyst). The ratio of water to silicon alkoxide (*R*) was either 2 or 4 (Table 2), and the methanol to TMOS ratio was varied between 2 and 4.5. After stirring for 40 min at 20 °C the appropriate lanthanide complex was added and the solution was stirred for between 1 and 6 h. Typical concentrations used were 15 mM for complexes [Tb.4] and [Tb.5], 7.5 mM for [Eu.3], and 5 mM for the others. Prior to spin-coating, the quartz substrates were placed overnight in concentrated HNO₃ and then cleaned sequentially using water and ethanol. Thin films were prepared by dropping 100 μ L of the sol solution onto one side of a rotating quartz disk. All films were spun at 2400 rpm using a Cammex Precima PRS14E spin-coater. After coating, all films were left at ambient laboratory conditions to stabilize for a period up to 28 days prior to analysis. This was to allow structural changes within the sol-gel matrix to evolve.²⁵ All membrane compositions are summarized in Table 2.

Instrumentation. The excitation and emission wavelengths used in this work are shown in Table 2, as are the excitation and emission slit widths. The optical system used to characterize the thin films is shown in Figure 3. For sol-gel matrixes doped with compounds [Tb.4], [Tb.5],

(25) McDonagh, C. M.; Sheridan, F.; Butler, T.; MacCraith, B. D. *J. Non-Cryst. Solids* **1996**, *194*, 72.

(26) Additional examples of the pH dependence of absorption, excitation, and emission spectra for [Eu3] (295 K, *I* = 0.1 M NaCl) are given as Supporting Information, together with the Eu-emission spectral profile and pH curve in human serum solution (λ_{exc} 365 nm, 298 K).

Table 2

film	TMOS/ acidified H ₂ O	TMOS/ MeOH	aging time (h)	stabilization time (days)	concn of complex (mM)	λ_{ex} (nm)	λ_{em} (nm)	ex slit (nm)	em slit (nm)
[Eu.1]	1/2	1/3.3	6	28	5	365	617	25	2
[Tb.1]	1/4	1/3	6	28	5	368, 311	544	3	1
[Tb.1]	1/2	1/3.3	6	28	5	368, 311	544	10	1
[Tb.2] ³⁺	1/4	1/3	6	28	5	365, 311	548	3	1
[Eu.3]	1/4 ^a	1/4.5	6	28	7.5	330	615	7	1
[Tb.4]	1/3 ^a	1/2.2	2	14	15	265	547	15	4
[Tb.5]	1/4 ^a	1/4.5	7	28	15	265	544	25	2

^a 0.04 M HCl (0.1 M HCl for films 1–4).

and [Eu.1], the coated substrate was mounted in flow cell A, which was illuminated at an angle of 35° to the excitation beam. All other films were characterized in the modified flow cell B, in which observation was at 90° to the centrally illuminated film. This geometrical setup exploits the anisotropic nature of fluorescence emission and uses internal reflection to capture and guide the emitted luminescence toward the detector. Emission slits as narrow as 1 nm were used, therefore increasing spectral resolution. Details of a similar optical setup can be viewed elsewhere.^{8a,22} Spectral artifacts such as second-order transmission and scattered excitation light were removed by using appropriate cutoff filters, although the latter could be observed in certain cases where flow cell A was used and requires a double emission diffraction grating to remove it from the emission optics. For response time and reversibility measurements, good signal-to-noise levels were achieved by using an increment of 2 s and 25 s, respectively, for the integration setting.

Buffer Solutions. Sulfonic acids (CHES, MOPS, and MES) were purchased from Sigma. The series of zwitterionic biological buffer solutions ranging from pH 5.5 to 10 (0.25–0.5 pH increments) were prepared at 0.1 M concentration of the free acid using NaOH to adjust the pH. The ionic strength was held constant at 100 or 20 mM using NaCl. HCl dilutions were used to set the pH below pH 5. Their ionic strength was set in the same way. Biological buffer solutions were pumped through the flow cell at a rate of 4 mL min⁻¹ using a peristaltic pump (Gilson). All buffer solutions were air saturated.

Acknowledgment. We thank the EPSRC and the BBSRC for grant support.

Supporting Information Available: Absorption emission and excitation spectra for complexes of **3** with Eu and Gd (6 figures). This material is available free of charge via the Internet at <http://pubs.acs.org>.

IC010371W